Engineering and Technology Journal
Journal homepage: https://etj.uotechnology.edu.iq

Drought forecasting model for future climate change effects in a regional catchment area in northern iraq

Nasser Kh. Muhaisen*, Thair S. Khayyun, Mustafa M. Al-Mukhtar

Civil Engineering Dept., University of Technology-Iraq, Alsina'a street, 10066 Baghdad, Iraq.
*Corresponding author Email: bce.19.82@grad.uotechnology.edu.iq

HIGHLIGHTS

- This study evaluated climate effects on Mosul Dam streamflow under 3 warming scenarios with 4 climate models.
- Findings projected temperature rise and diverse precipitation changes by 2100 based on scenarios.
- This research is the inaugural extensive examination of physical and meteorological traits in Iraq, Turkey, and Syria.

ARTICLE INFO

Handling editor: Mahmoud S. Al-Khafaji

Keywords:

Climate change

Tigris River

Streamflow

LARS-WG

SWAT model

ABSTRACT

Climate change plays a crucial role in shaping the hydrological dynamics of rivers owing to its immediate implications on the driving meteorological parameters. Therefore, Understanding climate change and its implications is essential for sustainable water resource management. This study aims to assess the extent of climate change and its effects on streamflow in the Mosul Dam watershed Under three global warming Representative Concentration Pathways scenarios (i.e., 2.6, 4.5, and 8.5) based on mean climate data extracted from four Global Circulation Models (i.e., Beijing Climate Center, China, Commonwealth Scientific and Industrial Research Organization, Australia, Met Office Hadley Center, United Kingdom, and Norwegian Climate Center, Norway). For this purpose, the stochastic weather generator model (LARS – WG) and soil and water assessment tool (SWAT) were used. The hydrological model (SWAT) was calibrated and validated for 2001-2013 and 2014-2020, respectively. The performance of the swat model according to the four statistical parameters (i.e., coefficient of determination, Nash-Sutclife, Root mean square error to the standard deviation, and percent bias test) was classified as very good for two calibration and validation processes. Additionally, results showed that the mean temperature would probably rise by 1.3, 2.4, and 4.5°C under RCP 2.6, RCP 4.5, and RCP 8.5 at the end of this century, respectively. At the end of the century, the simulated average annual precipitation decreased from 772 mm/y to 756.7 and 741.6 mm/y under RCP4.5 and RCP8.5, respectively. In contrast, under the RCP2.6 scenario, the mean annual precipitation increased to 803 mm/year. As a result, the projected mean annual streamflow decreased from 501.52 m^3/s to 429.7, 391.9, and 376.6 m^3/s at the end of the century under RCP2.6, RCP4.5, and RCP8.5, respectively. Finally, the study region will potentially face water shortage due to climate change, exacerbated by population growth and increased water demands from agriculture and municipalities. Therefore, this paper emphasizes the need for reevaluating and adapting to accommodate changing streamflow patterns, ensuring a sustainable water supply for human needs while protecting the environment.

1. Introduction

Climate change poses a worldwide challenge, impacting various aspects of life, including water resources. The emission of greenhouse gases, predominantly caused by human activities, contributes significantly to global warming, consequently affecting social and natural systems through climate alterations. The hydrological system is an essential component of the climate regime. As such, the negative consequences of climate change primarily manifest in water resources by disrupting the hydrological cycle through changes in evapotranspiration and precipitation patterns [1,2].

In the late 20th century, the World Climate Research Program (WCRP) established the Coupled Model Intercomparison Project (CMIP) to facilitate climate change investigation. CMIP5, proposed by the WCRP, has become a commonly employed

http://doi.org/10.30684/etj.2024.144458.1634
Received 07 November 2023; Received in revised form 07 January 2024; Accepted 07 January 2024; Available online 20 January 2024
2412-0758/University of Technology-Iraq, Baghdad, Iraq

framework for analyzing the trends and attributes of future climate change [3]. Currently, the Representative Concentration Pathways, i.e., RCP 2.6, RCP 4.5, and RCP 8.5 scenarios within CMIP5, are extensively utilized as climate simulation prediction models [4].

Global Climate Models (GCMs), or atmospheric circulation models, effectively project climate trends for future periods. However, these models suffer from low spatial resolution, typically around 200 km × 200 km, which limits their ability to provide detailed information at regional scales. Additionally, the output data generated by different GCMs are large-scale grid data, leading to a lack of precision in predicting regional climate scenarios [5]. Hence, downscaling methods are necessary to achieve more accurate regional climate scenarios [6]. There are two frequently employed software tools for climate predictions and the downscaled analysis of past and future climate data: the Stochastic Weather Generator (LARS-WG) and Statistical Downscaling Models (SDSM) [7]. Statistical Downscaling Models (SDSM) can also analyze past climate data. The Long Ashton Research Station Weather Generator LARS-WG model is a random weather generator. It is one of the most widespread models created to assess the effects of climate change. It has been committed to investigating various environmental circumstances, during which it has performed admirably compared to other generators [8]. Numerous investigations have been carried out to simulate various climatic variables such as air temperature, precipitation, and runoff using the combined approach of LARS-WG and GCMs [9-12].

Hydrological models are utilized to simulate future water cycles, with Global Climate Models (GCMs) providing projected precipitation and temperature data to drive these models. The choice of an appropriate hydrological model depends on factors such as the spatial scale of the model, basin characteristics, data availability, desired accuracy, research objectives, and ease of calibration [13]. However, the effectiveness of hydrological models decreases in basins with high elevations and limited measurement data, mainly when snowmelt significantly contributes to the water flow [14]. Hence, estimating runoff in such catchments poses significant challenges owing to the configuration of the catchment's constraints.

In recent years, many hydrologic models have been developed, each with unique structural characteristics. Semi-distributed models, out of all the many types of models, are normally the most successful for hydrological modeling. This is because semi-distributed models avoid problems commonly encountered with entirely distributed models and lumped models [15]. A prime instance of such a model is the Soil and Water Assessment Tool (SWAT), a commonly used model. The model is a complete, physically grounded parameter model that necessitates a multitude of input factors, including soil characteristics, topographical features, and plant characteristics [16]. The USDA Agriculture Research Service developed the method to assess the impact of land management strategies throughout extensive and intricate watersheds [17]. The SWAT model is extensively used in hydrologic research to evaluate and forecast both surface and subsurface flow patterns [18-22], a consideration of the consequences that climate change would have on streamflow [1,23,24] and the assessment of water quality [25,26], including nutrient loading, total daily peak concentrations, pesticides, and microorganisms. The SWAT hydrological model may be used not only in arid areas but also in semi-arid and humid regions, such as India, as described by Li and Fang [27], Tunisia, as described by Hemrassi et al. [28], Ghana, as described by Samuel et al. [29], and Laos, as described by Vilaysane et al. [30].

Iraq's water resources have significantly reduced over the last several decades. The water shortage situation in Iraq has been influenced by various factors, including the water policies implemented by surrounding nations, the impact of recent climatic changes, and the inadequate management of water resources inside the country. This mismanagement encounters challenges, including heightened water demand resulting from rapid population expansion, elevated river sediment levels, and the disregard for sanitation infrastructure. Consequently, improperly mixing wastewater with rainwater and subsequent direct discharge into rivers leads to pollution and degradation of their overall quality [31].

The Tigris River upstream of Mosul Dam in Iraq has little attention concerns with the impact of climate change on the water resources that enter the reservoir. To the best of my knowledge, limited studies were conducted to assess the water scarcity in the catchment. Further research is required to comprehensively understand the future water resources in the Mosul Dam Watershed, particularly in the context of global warming. This knowledge is crucial for developing effective strategies and plans to ensure the sustainable management of water resources in the region. Hence, the present study seeks to examine the ramifications of global warming on the forthcoming trajectory of the climatic and hydrological systems inside the Mosul Dam Watershed. As such, the study emphasizes the role of the watershed's temperature, precipitation, and streamflow as configuring parameters in shaping the water availability of the catchment.

This study is the first thorough hydrological dynamics examination of the Mosul dam watershed, including the physical and climatic attributes of the surrounding riparian watersheds in Turkey and Syria, which distinguishes it from earlier research. To achieve the objective, the minimum and maximum temperatures and precipitation data collected from eight climate stations during the reference period of 2001–2020 were used. These recorded values were then projected into four future periods: 2021-2040, 2041-2061, 2061-2080, and 2081-2100. The LARS-WG model was employed with four Global Climate Models (GCMs) and three Representative Concentration Pathways (RCPs) to carry out these projections. In addition, the researchers used the existing and anticipated climatic data to establish a SWAT-based model for evaluating the streamflow inside the Mosul Dam watershed.

2. Material and methods

In this study, material and methods are divided into six sub-divisions, including the study area, data collection, methodology, SWAT model description, and criteria for evaluation of the SWAT model and presented as follows:

2.1 Study area

The Tigris River spans a length of over 1800 kilometers and has its source in the Taurus Mountains, located in the eastern region of Turkey. The geographical location of the area in question is around 25 kilometers southeast of Elazig, with an

additional proximity of around 30 kilometers from the origin of the Euphrates River. As shown in Figure 1, the watershed of the Tigris River that is situated upstream of the Mosul dam has an estimated area of 54,300 km^2 and is divided into three different regions. The upper stretch of the river can be found located upstream of the Illisu dam, while the middle section of the river can be found between the Illisu dam and the proposed Cizre dam [32]. In conclusion, the lower part may be found near the Cizre and Mosul dams. This research focused primarily on the southern section of the area included by the Iraq-Turkey-Syria borders, as seen in Figure 1. Specifically, the study examined the region between the latitudes of 36º35′20″ and 37º48′00″ N and the longitudes of 41º46′33″ and 43º29′17″ E. The Mosul Dam is among the largest dams in Iraq. The location in question is situated 52 kilometers upstream of Mosul city, namely on the Tigris River, inside the western province of Nineveh [32]. The primary objectives of the dam are to facilitate the storage of surplus water for flood control, agriculture, and electricity production. The yearly generation of electrical power amounted to 1060 MW, while the historical data on water flow into the reservoir indicated that the highest, lowest, and average monthly inflow between 2001 and 2020 were around 2881, 77, and 477 m^3/sec, respectively. In this region, temperature records from climate stations indicate that the highest temperature was 46ºC, observed in August, whereas the lowest temperature was recorded in January. The rainy season in this area typically commences in October and lasts until May. Furthermore, the annual rainfall in this region exceeds 1000 mm [33].

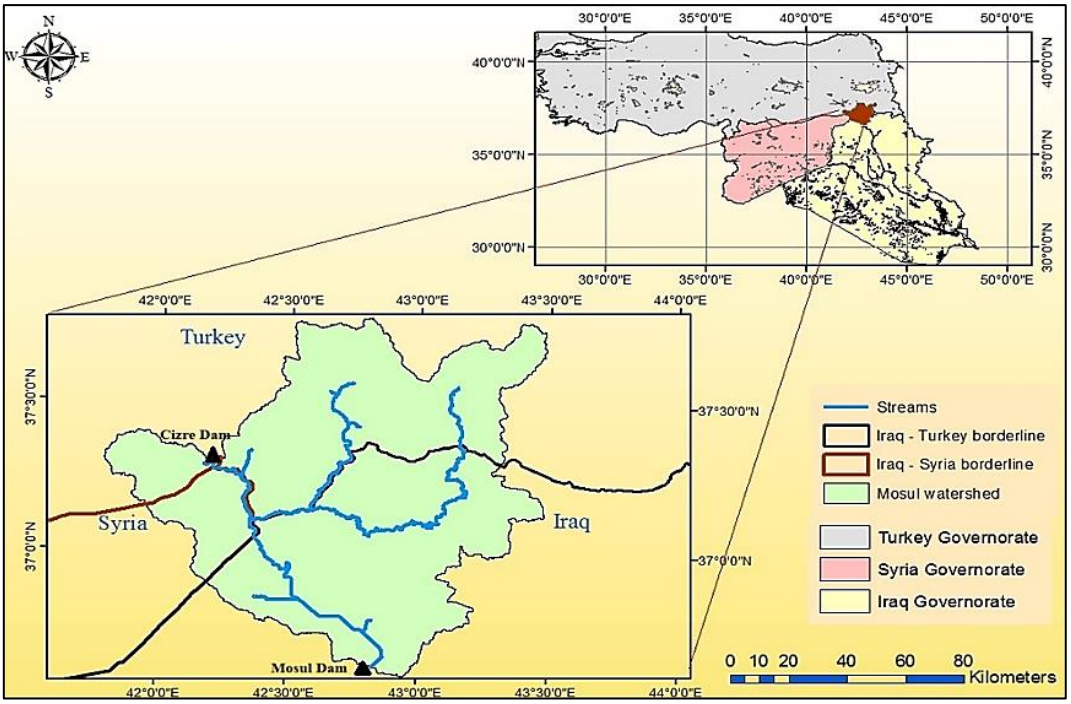

Figure 1: Location of Mosul Dam Watershed

2.2 Data

2.2.1 Meteorological data

The historical daily weather data were downloaded from the selected eight meteorological stations across the watershed in Turkey and Iraq from 2001-2020, as illustrated in Table 1. The five weather data sources are provided by the Climate Hazards Group Infrared Precipitation with Station data (CHIRPS) and the National Aeronautics and Space Administration (NASA), respectively.

Table 1: Geographical coordinates of the selected meteorological stations

Station No.	Lat.	Long.	Length of Record	Location
1	37º08′00	42º43′12″	2001-2020	Iraq
2	36º52′12″	43º00′00″	2001-2020	Iraq
3	37º15′36″	43º10′00″	2001-2020	Iraq
4	37º30′00″	42º54′00″	2001-2020	Turkey
5	37º24′00″	42º30′00″	2001-2020	Turkey
6	37º12′00″	42º24′00″	2001-2020	Turkey
7	36º57′00″	42º30′00″	2001-2020	Iraq
8	36º42′00″	42º45′00″	2001-2020	Iraq

2.2.2 Digital elevation data

This study used the Shuttle Radar Topography Mission (SRTM) version 3.0's digital elevation model (DEM) with a spatial resolution of 30 m (1-acre-second) to delineate the watershed of the Mosul dam, extract streams, and calculate sub-basins as in

source [34]. This information is visually shown in Figure 2. The Shuttle Radar Topography Mission (SRTM) dataset was obtained from the open topography website (https://portal.opentopography.org) in June 2022. The data was downloaded in a TIF file and first stored in the geographic coordinate system. Subsequently, the dataset was transformed and projected into the Universal Transverse Mercator (UTM) coordinate system. The catchment area included 11,108 square kilometers, with Iraq accounting for 48% of this area, Turkey for 44%, and Syria for 8%.

2.2.3 Land use and soil data

The land use/land cover map was downloaded from the climate data store website (https://land.copernicus.eu/global/.) for the year 2015, which has been defined using the United Nations Food and Agriculture Organization's (UN FAO) Land Cover Classification System (LCCS) with a spatial resolution of 100 m. The land cover in the watershed of Mosul Dam can be classified into seven distinct classes, as depicted in Figure 3. The major parts of the watershed's land use were pasture (52.26%) and agricultural land (36.15%).

The study region's soil classification map was created using the Food and Agriculture Organization of the United Nations soil classification system's worldwide soil dataset (Fao, 1995), which provides data for over five thousand soil varieties at a one-to-five-million-scale In watershed modeling, soil type affects hydrological processes. FAO-UNESCO soil categorization comprised soil texture, accessible water content, bulk density, organic carbon content, and hydraulic conductivity (Fao, 1995). Before being included in the ArcSWAT2012 model for modeling, these characteristics must be examined. Figure 4 and Table 2 demonstrate that 48.15%, 16.96%, and 34.89% of the Mosul Dam watershed's soil were loam, clay loam, and clay soil, respectively.

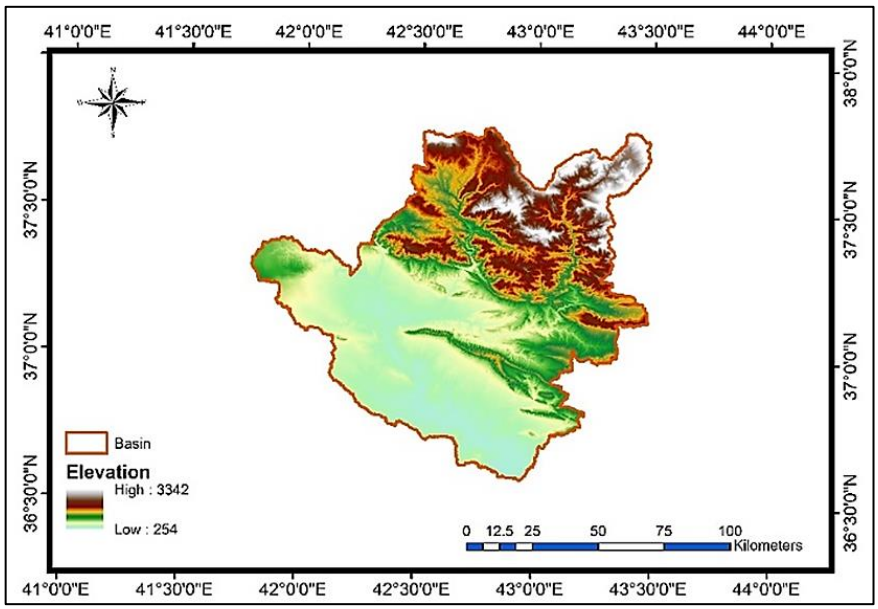

Figure 2: Digital elevation map for Mosul dam watershed

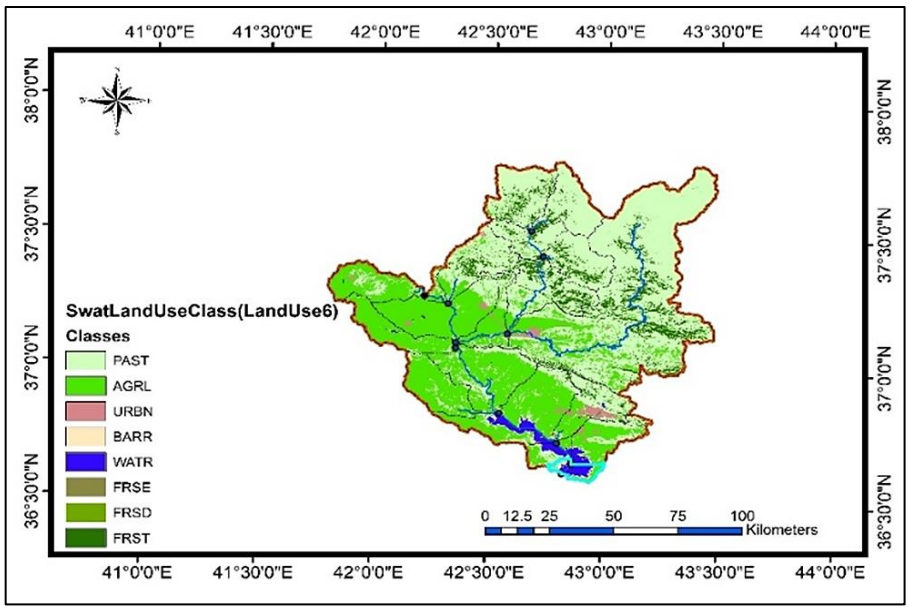

Figure 3: LU/LC map of Mosul dam watershed

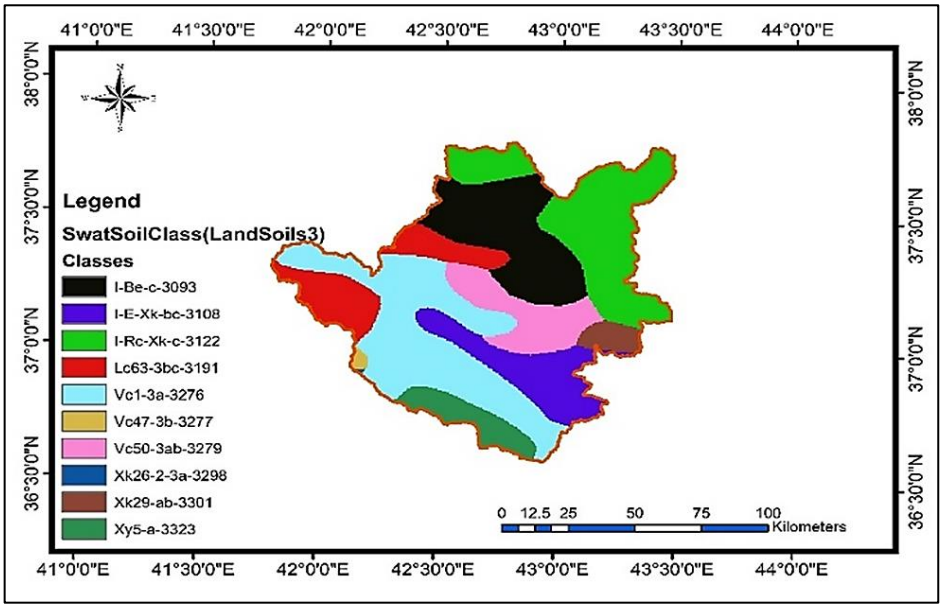

Figure 4: Soil classification of Mosul Dam watershed

Table 2: Soil types and Coverage area for the Mosul Dam watershed

SWAT Soil Class	Soil type	Hydrologic Group	of watershed area%	Area (Km^2)
I-Be-c-3093	Loam	D	16.92	1880
I-E-Xk-bc-3108	Loam	D	10.39	1154.4
I-Rc-Xk-c-3122	Loam	D	20.84	2314.8
Lc63-3bc-3191	Clay-Loam	D	9.65	1072.3
Vc1-3a-3276	Clay	D	25.74	2859
Vc47-3b-3277	Clay	D	0.40	45
Vc50-3ab-3279	Clay	D	8.75	971.6
Xk26-2-3a-3298	Clay-Loam	D	0.04	4.24
Xk29-ab-3301	Clay-Loam	D	2.23	247.6
Xy5-a-3323	Clay-Loam	D	5.04	559.3

2.2.4 Streamflow data

Al Dabbagh [35] and the Ministry of Water Resources/ General Directorate of Dams and Reservoirs provided the monthly inflow data for the Mosul Dam reservoir. Figure 5 illustrates the average monthly point source discharge to the watershed in the SWAT model for the period (2001-2020), which was derived based on the average monthly flow recorded at the Cizre gauge station. This gauge station is situated upstream in the Mosul watershed.

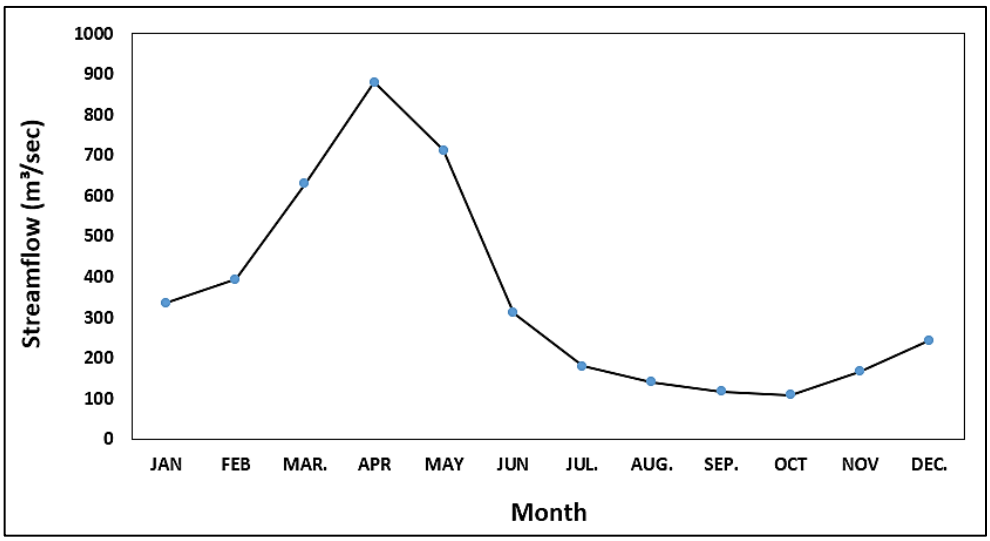

Figure 5: Average monthly streamflow at Cizre station from 2001-2020

2.3 Representive concentration pathways scenarios

Four scenarios RCPs (Representative Concentration Pathways), namely 2.6, 4.5, 6.5, and 8.5, were established to represent different radiative forcing levels, ranging from 2.6 to 8.5 W/m^2. The radiative forcing magnitude depends on carbon dioxide emission levels [36]. This study utilized three RCP scenarios (RCP2.6, RCP4.5, and RCP8.5) representing low, medium, and high socioeconomic developments. These three scenarios have been widely employed in numerous studies assessing the impacts of climate change [3,38]. Four GCMs (i.e., BCC- CSM1-1, CSIRO_MK3.6, HaDGEM2-ES, and NorESM1-M) were chosen depending on the previous literature to reduce the uncertainty in projected climate data.

As stated previously, the output of GCM models has little resolution and cannot be directly applied to the hydrological model. In this study, the LARS-WG model was chosen to downscale the output of the Four GCMs model for the period (2021-2100). The LARS-WG model has been effectively utilized in various water resource applications with a positive outcome [39,40]. This model utilized a semi-empirical distribution to generate future weather time series by statistically analyzing records from a single weather station.

2.4 Swat model description

Soil and Water Assessment Tool (SWAT) is a comprehensive, physically based parameter that requires a lot of input parameters such as soil information, topography, and vegetation nature [41]. It was developed by the USDA Agriculture Research Service to measure the effect of land management techniques in sizable, complicated watersheds [42]. Using spatial datasets, SWAT divides the main basin into many subbasins, and each subbasin is subsequently divided into smaller units called Hydrologic Response Units (HRUs) that contain unique combinations of topography, LULC, and soil characteristics. Hydrologic simulation of any basin in the Soil and Water Assessment Tool passes through two phases. Firstly, in the land phase, the runoff is calculated based on the water balance equation for each Hydrologic Response Unit level as in Equation (1), and the results are combined for the basin [22].

$$\mathrm{SWt} = \mathrm{SWo} + \sum_1^t (R_{day} - Q_S - E_a - W_S - Q_{gw}) \quad (1)$$

Where SWt represents the water content of the soil in (mm), SWo represents the initial water content in soil (mm), t the time (day), Rday is the daily rainfall in (mm), Ea the evapotranspiration (mm), Ws represents the water stored in vadose (mm), Qg The amount of water returning from the ground to the surface (mm), and Qs represents the surface runoff (mm) that is calculated based on Soil Conservation Service Curve Number method (SCS-CN). This method calculates the volume of runoff and peak value of surface runoff for each Hydrologic Response Unit as:

$$\mathrm{Er} = \frac{(R-0.2r)^2}{(R-0.8r)} \quad (2)$$

Er Excess rainfall is measured in (mm), and the retention parameter (r) is measured in millimeters. The retention parameter (r) is defined as follows and has the following correlation with the curve number of the average moisture condition for the day (CNII):

$$\mathrm{r} = 25.4\left(\frac{1000}{CN_{II}} - 10\right) \quad (3)$$

Secondly, the SWAT model undertakes flow routing in the context of flow within channels and reaches. This involves predicting downstream water movement within channels or reaches. This prediction can be based on the variable storage coefficient method [43] or the Muskingum routing method. These approaches are routed in kinematic wave models.

Soil and Water Assessment Tool calibration and uncertainty program (SWAT-CUP) was employed with the semi-automated global search procedure, i.e., the Sequential Uncertainty Fitting version 2 (SUFI-2) algorithm, to calibrate and validate the SWAT model. This algorithm is characterized by achieving calibration results faster than the remainder of the algorithms included in this program, such as particle swarm [44].

Parameter uncertainties in a SUFI-2 calibration/uncertainty analysis encompass uncertainties from driving variables like rainfall, the model itself, parameters, and measured data such as flow. The effectiveness of accounting for these uncertainties is determined using the P-factor (percentage of measured data within the 95% prediction uncertainty, 95PPU) and the R-factor (ratio of average 95PPU band thickness to the standard deviation of measured data). These measures collaboratively minimize the uncertainty band to encompass a significant portion of measured data. Calibration aimed to derive optimal runoff parameters.

2.5 Methodology

This study calibrated and validated the SWAT model against the measured monthly inflow data into the Mosul Dam Reservoir. The model was set up using the relevant climate data of the base period of 2001-2020. After that, the LARS-WG was employed to downscale the future climate data up to 2100 from four Global Climate Models (BCC- CSM1-1, CSIRO_MK3.6, HaDGEM2-ES, and NorESM1-M) under three different RCP scenarios, i.e., RCP2.6, RCP4.5, and RCP8.5, respectively. The average downscaled climate data were fed into the calibrated SWAT model to assess the availability of water resources during four different future periods (2021-2040, 2041-2060, 2061-2080, and 2081-2100).

2.6 Evaluation criteria

Four statistical criteria were used to evaluate the effectiveness of the Soil and Water Assessment Tool (SWAT) model simulation of the Mosul Dam Reservoir watershed. The ratio of the Root Mean Square Error (RMSE) to the standard deviation of observed data (STDobs) (RSR), the percent bias (Pbias), the Nash-Sutcliffe efficiency (NSE), and the coefficient of determination (R^2) were among the criteria used.

Nash-Sutcliffe efficiency (NSE) quantifies the degree to which the simulated value predicts the component of interest better than the mean observed value, with an NSE value of 1 showing ideal modeling. The NSE value ranges from (-∞) to 1, with values greater than or equal to 0, pointing to the replicated value predicting the component of interest with greater precision than the mean observed value. The NSE values were calculated using the following Equation:

$$N_{SE} = 1 - \frac{\sum_{i=1}^{N}(Q_i - M_i)^2}{\sum_{i=1}^{N}(Q_i - Q_a)^2} \quad (4)$$

The variables Qi and Mi represent the observed and simulated stream flow values for the ith pair of stream flow values. Qa denotes the mean value of the observed stream flow values, whereas N represents the total number of paired stream flow data.

The root mean square error ratio to the observed data's standard deviation is a statistical measure used to evaluate a model's or prediction's accuracy. The simulation will take input values of RSR that are below 0.5. The aforementioned equation was used to compute the RSR values:

$$RSR = \frac{RMSE}{STD_{ob}} = \frac{\sqrt{\sum_{i=1}^{N}(Q_i - M_i)^2}}{\sqrt{\sum_{i=1}^{N}(Q_i - Q_a)^2}} \quad (5)$$

The percent bias test is used to ascertain whether or not the general trend of the modeled data is more or less than that of the data that has been observed. If the Pbias values are zero, the modeled data is superior to the real data on average. On the other hand, negative numbers suggest that the average of the modeled data is lower than the average of the observed data. When the value of Pbias is equal to zero, the simulation will behave in the expected way and display the usual features. The values for Pbias were derived by applying the following equation to the data:

$$P_{bias} = \frac{\sum_{i=1}^{N}(Q_i - M_i)}{\sum_{i=1}^{N} Q_i} \quad (6)$$

The coefficient of determination, often known as R^2, is a statistical tool that evaluates how effectively a model replicates observed data based on the percentage of the total variance accounted for. R^2 values may vary from 0 to 1, with closer to 1 indicating greater model performance. The range of R^2 values can be thought of as a continuous scale. To compute the R^2 values, the following Equation was utilized:

$$R^2 = \frac{[\sum_{i=1}^{N}(Q_i - Q_a)(M_i - M_a)]^2}{\sum_{i=1}^{N}(Q_i - Q_a)^2 \sum_{i=1}^{N}(M_i - M_a)^2} \quad (7)$$

where Ma The mean value of the modeled stream flow.

3. Results and discussion

3.1 Future trends in climate variables

The anomaly of the downscaled monthly temperature and precipitation data from the ensemble mean of the GCMs under three RCPs scenarios of the eight stations across the Mosul dam catchment area compared to the future evaluated periods were plotted as shown in Figures 6 and 7. As can be seen from Figure 6 (a-f), there is an increasing trend in temperatures averaged over the entire basin. The higher increase was noticed under RCP 8.5. At the same time, the lowest increase was obtained from RCP2.6.

From Figure 6, the lowest difference (increase) in minimum and maximum temperatures occurred in December for all future periods under three greenhouse gas emission scenarios. On the other hand, the highest increase in minimum and maximum temperatures fluctuated between May and July for all future periods under three different scenarios. These results were consistent with the results presented by Saeed [45] and Haithem and Al-Mukhtar [46].

Figure 7 (a-c). shows the future trend in precipitation. The future trend in the predicted precipitation for the Mosul Dam watershed was generally decreased. For example, under all three scenarios, the highest decrease in precipitation occurred in May for future periods (i.e., 2021-2040,2041-2060, 2061-2080, and 2081-2100), respectively. However, a significant increase in predicted precipitation over the Mosul Dam watershed under RCP2.6 and RCP8.5 reached 20% and 15% for the same future period (2021-2040), respectively.

3.2 Sensitivity analysis of swat model

Twenty hydrological factors were examined to identify the key parameters that contribute to the accurate modeling of stream flow in the watershed of the Mosul reservoir dam. Sequential Uncertainty Fitting version 2 (SUFI2) method, a semi-automated global search process, was utilized in the calibration and uncertainty program of the Soil and Water Assessment Tool (SWAT). Based on the statistical parameters, namely the p-value and t-stat value, it was observed that six hydrological parameters exhibited significant sensitivity in the calibration of the Mosul Dam reservoir watershed model. These findings are shown in Table 3. Parameters were deemed to possess significant sensitivity when the P-value was below 0.1. The most sensitive parameters were the curve number factor (CN2), the baseflow alpha factor (ALPHA_BF), the effective hydraulic conductivity in main channel alluvium (CH_K2), the soil available water capacity (SOL_AWC), the snowfall temperature (SFTMP), and the snowmelt base temperature (SMTMP).

Table 3: Watershed sensitivity analysis of the Mosul Dam Model parameters for runoff calibration.

Parameter	Rank	P - Value	t- value	Initial values	Final values	Fitted value
ALPHA_BF	1	0.00	16.9	0– 1	0.12 - 0.87	0.69
SMTMP	2	0.00	-13.68	-5 - 5	-3.1 - 3.6	2.66
CN2	3	0.00	-7.3	-0.3 - 0.3	-0.15 – 0.03	-0.10
SFTMP	4	0.00	-5.78	-5 - 5	-3.23 - 3.96	9.39
SOL_AWC(..)	5	0.02	2.24	-0.5 – 0.5	-0.12 - 0.33	0.10
CH_K2	6	0.04	-2.03	100-200	115.24- 155.62	147.27

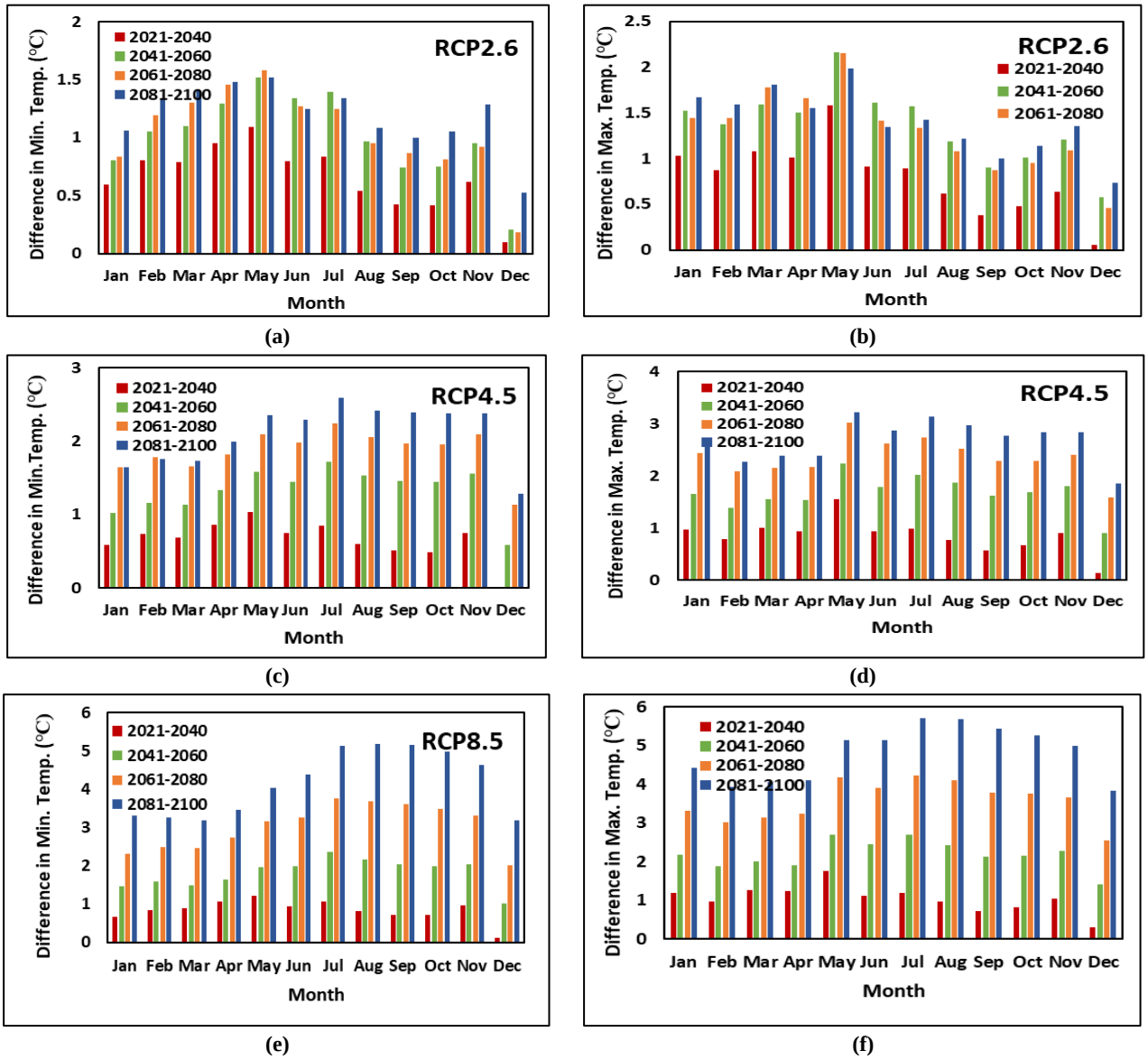

Figure 6: Future Differences in Min and Max. Temperatures for the Mosul Dam watershed under three scenarios (a): Difference in Min. Temp under RCP2.6, (b) Difference in Max. Temp under RCP2.6, (c): Difference in Min. Temp under RCP4.5, (d): Difference in Max. Temp under RCP4.5, (e): Difference in Min. Temp under RCP8.5, and (f): Difference in Max. Temp under RCP8.5

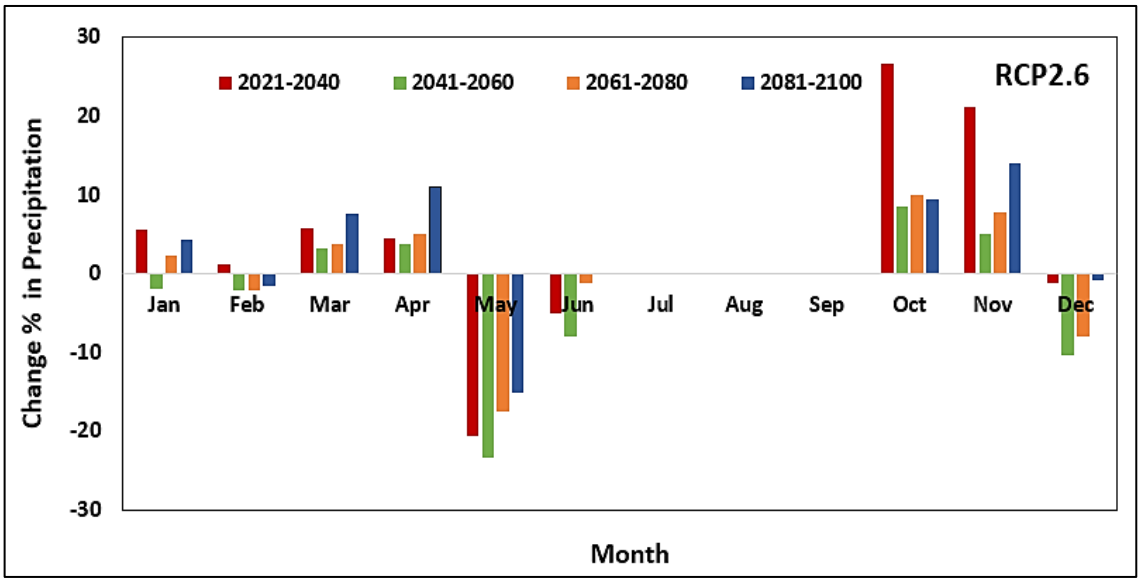

(a)

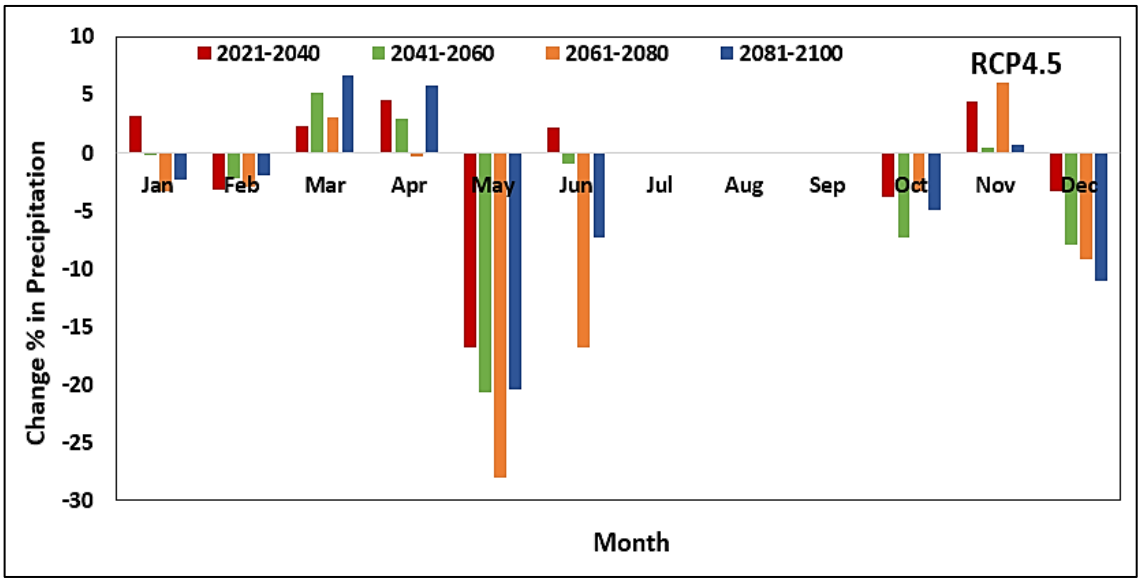

(b)

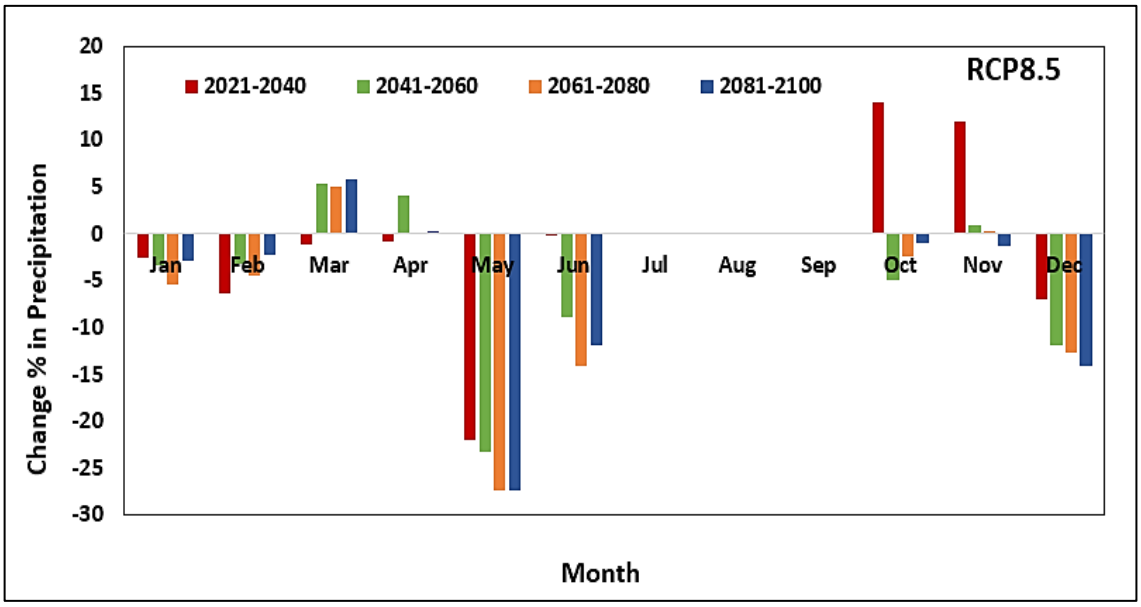

(c)

Figure 7: Future trend in precipitation for Mosul Dam watershed under different scenarios, (a): RCP2.6 Scenario, (b): RCP4.5 Scenario, and (c): RCP8.5 Scenario

3.3 Calibration, validation, and model performance

The SWAT model was calibrated and validated against the measured monthly inflow data into the Mosul Dam Reservoir, spanning from 2001 to 2020. The streamflow data collected from 2001 to 2013 were used for calibration purposes, whereas the data from 2014 to 2020 were employed for validation. The SWAT-CUP software was executed many times throughout the calibration process, including 700 simulations for each iteration. The calibrated parameter ranges were selected based on the results obtained from the last iteration, as seen in Table 3. The results of Nash-Sutclife (N_{SE}) and Coefficient of determination (R^2) for calibration and validation processes were consistent with the results of the monthly runoff simulation on different studied watersheds conducted by various researchers such as Al-Kaky et al. [22], Wu and Chen. [47], and Robert et al. [48].

The validation procedure was conducted using the same parameters, without altering their ranges, and with a consistent number of simulations. Figures 8 and 9 depict the streamflow time series over the calibration and validation period, showcasing the measured and simulated data. Additionally, Figures 9a and 9b illustrate the correlation between the measured and modeled streamflow for two consecutive periods (calibration and validation).

To determine whether or not the SWAT model for the Mosul Dam watershed is accurate, it was required to use the parameters for statistical analysis provided by Moriasi et al. [49]. This was the case. Calculations for the present and the past were used to analyze these variables, as evidenced by Table 4, which displays the results. Based on the values of these parameters, it was determined that the accuracy of the Mosul Dam Reservoir catchment model was extremely high during both the calibration and validation periods.

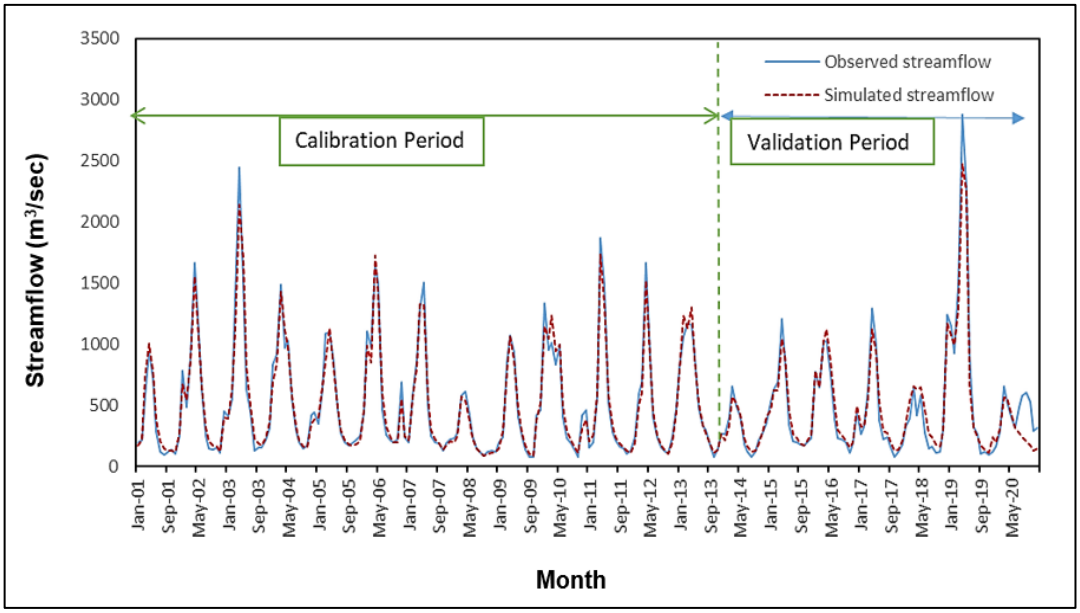

Figure 8: Observed and Modeled streamflow time series for Mosul Dam watershed

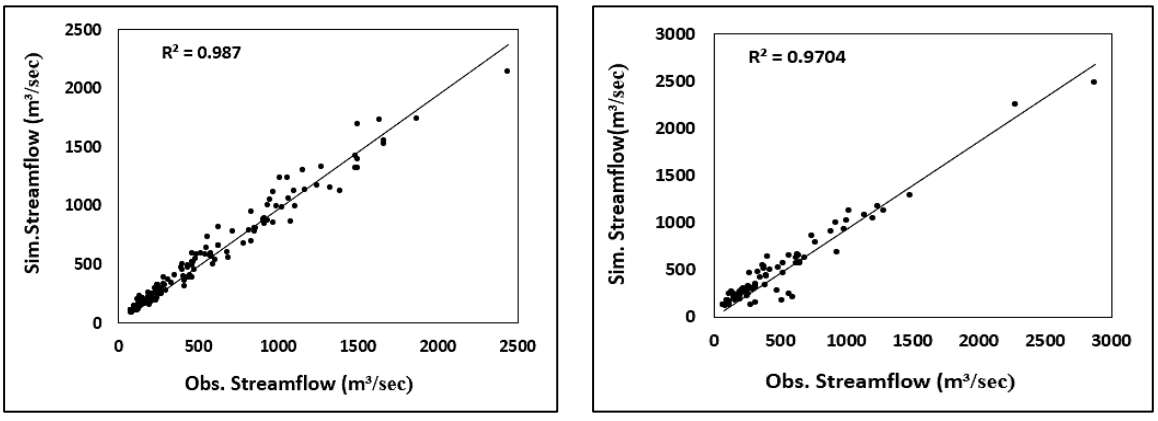

(a) **(b)**

Figure 9: Relationship between Observed and Simulated stream flow for (a) Calibration period, (b) Validation period

Table 4: Statistical parameters for calibration and validation periods

Period	N_{SE}	R^2	RSR	P_{bias} (%)
Calibration period (2001 – 2013)	0.97	0.97	0.17	0.1
Validation period (2014 – 2020)	0.94	0.93	0.26	1.8

3.4 Future trend of streamflow

The calibrated SWAT model was further employed to assess the future behavior of the Mosul dam catchment area using climate data from four GCMs. The anomaly of the monthly future streamflow concerning the baseline period was calculated. The results of the future average monthly streamflow under three RCP scenarios are shown in Figure 10 (a-c). The average data of the global circulation models were considered in calculating the streamflow of the Mosul Dam watershed to avoid biased results in some models. The mean annual streamflow of the watershed in the baseline period was 501.52 m^3/sec, with a peak value of 1253.3 m^3/sec in April. As such, the mean annual streamflow tends to decrease to 438.2, 399.7, 410.4, and 429.7 m^3/sec under the RCP2.6 scenario for 2021-204, 2041-2060, 2061-2080, and 2081-2100, respectively. Similarly, the decrease in mean annual streamflow will be more noticeable under the RCP4.5 scenario (i.e., 409.6, 397.5, 390.5, 391.9 m^3/sec for 2021-204, 2041-2060, 2061-2080, and 2081-2100, respectively). Additionally, under RCP8.5 scenarios, the mean annual streamflow tends to decline to 398.4, 391, 376.4, and 376.6 m^3/sec for 2021-204, 2041-2060, 2061-2080, and 2081-2100, respectively.

The future monthly streamflow changes in the Mosul Dam watershed under three RCP scenarios are shown in Figure 11 (a-c). The highest decrease in streamflow occurred in November under three scenarios for all future periods. Conversely, the smallest decrease in streamflow exhibited variability across all scenarios considered in this study throughout future periods. The results of this study were consistent with the results in [46].

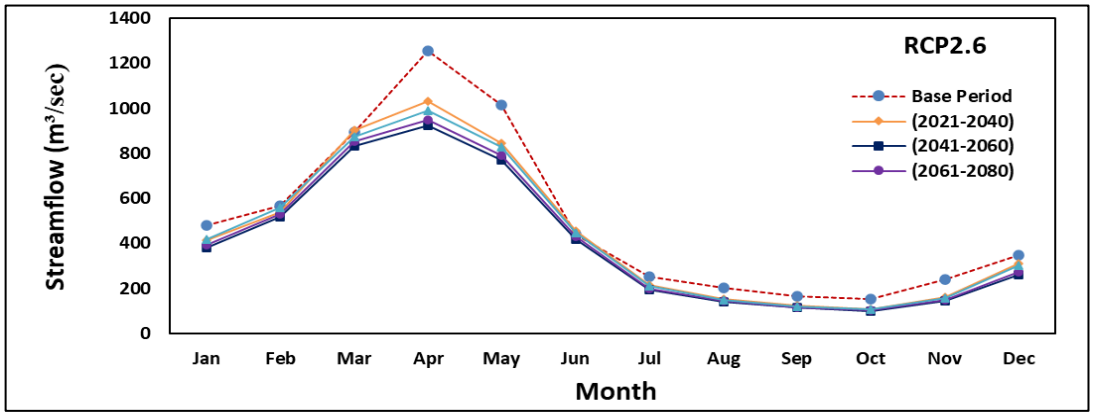

(a)

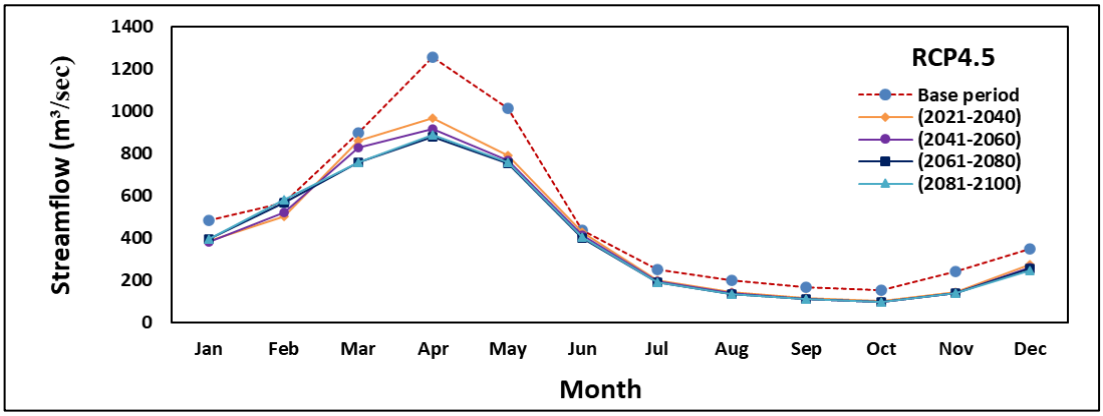

(b)

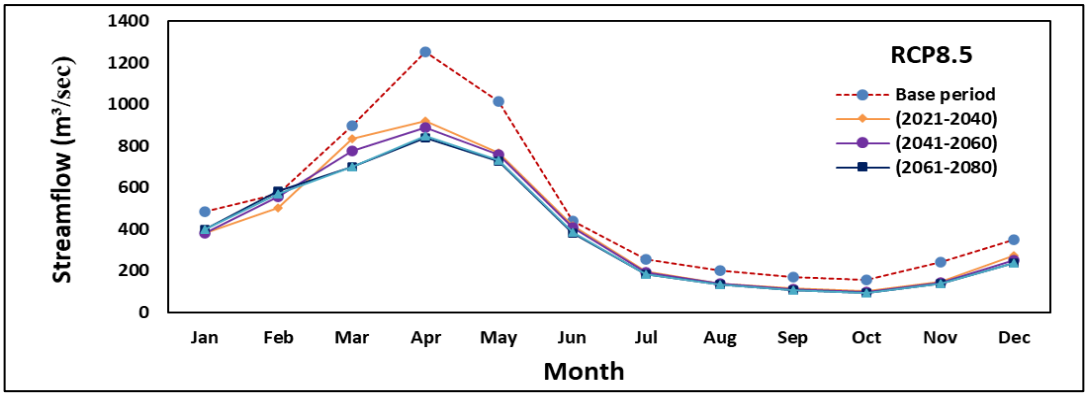

(c)

Figure 10: Mean monthly simulated future streamflow under different scenarios of global warming, (a): RCP2.6 Scenario, (b): RCP4.5 Scenario, and (c): RCP8.5 Scenario

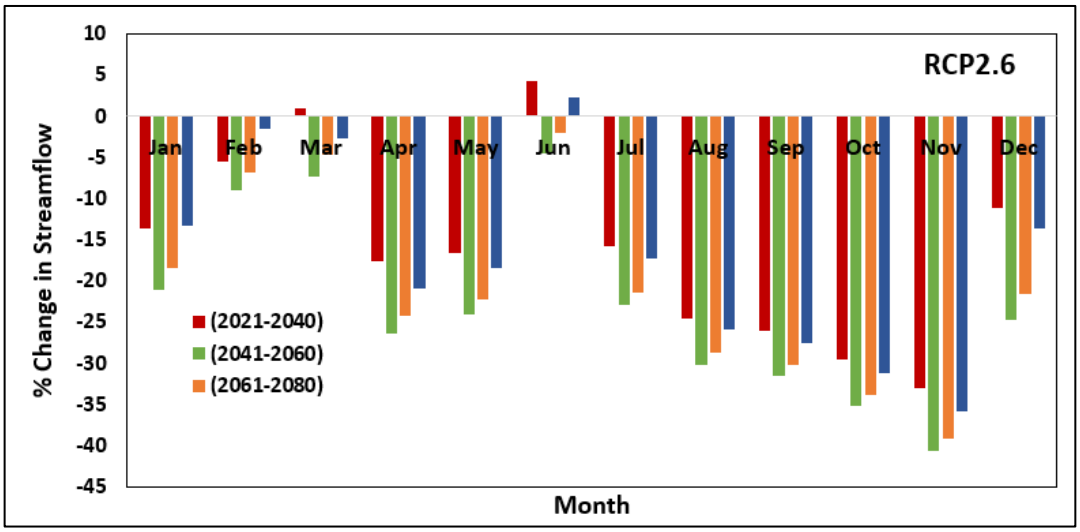

(a)

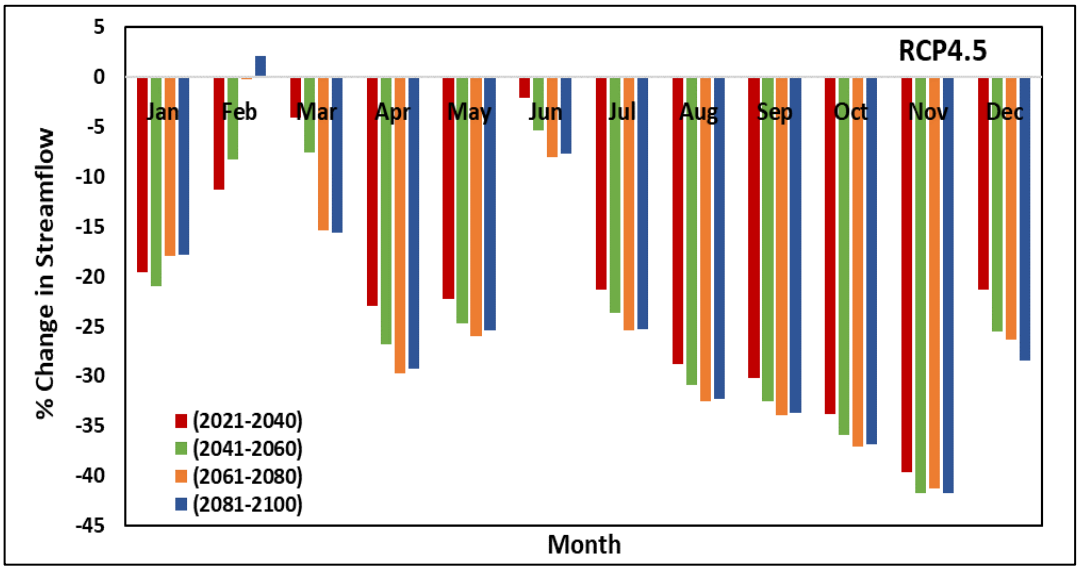

(b)

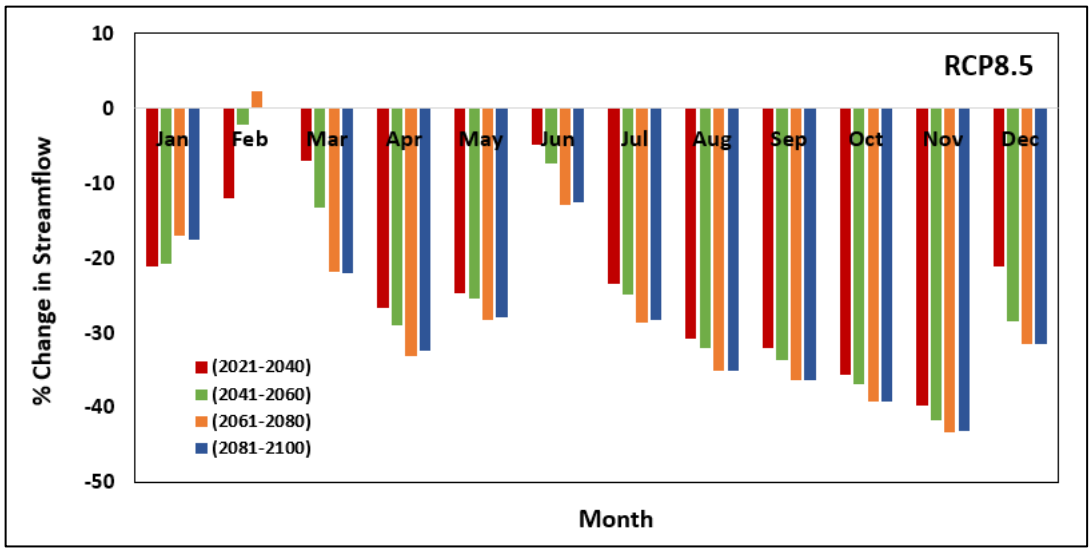

(c)

Figure 11: Monthly Change in future streamflow under different global warming scenarios,(a):RCP2.6 Scenario, (b): RCP4.5 Scenario, and (c): RCP8.5 Scenario

4. Conclusions and Recommendations

This study investigates the relationship between the impact of climate changes and streamflow in the Mosul Dam watershed over four periods, i.e., 2021-2040, 2041-2060, 2061-2080, and 2081-100, considering three global warming scenarios (three Representative Concentration Pathways (RCPs), 2.6, 4.5, and 8.5) of four global circulation models were ensemble to assess the future water resources behavior of the catchment. To this end, the SWAT model coupled with the statistical downscaled climate data from the LARS-WG was run, and the results were compared to the baseline period of 2001-2020. According to the results of this study, the most important conclusions are:

1) Mosul Dam watershed has suffered from high dryness and temperatures at the end of the century due to climate changes induced by global warming.
2) Due to the decrease in rainfall at the end of the century under climate change scenarios, the study proved that there would be a significant decrease in the expected streamflow.
3) The study also highlights the substantial influence of CN2, groundwater, soil, and snow parameters on streamflow in watersheds, being the most sensitive parameter affecting the hydrological behavior of the catchment.
4) The watershed will face a water shortage due to climate change, exacerbated by population growth and increased water demands from agriculture and municipalities. Therefore, this paper recommends reevaluating and adapting the plans for water resource management to accommodate the changes in streamflow patterns and ensure a sustainable water supply for human needs while protecting the environment.

Author contributions

Conceptualization, N. Muhaisen, T. Khayyun, and M. al-Mukhtar; methodology, N. Muhaisen, T. Khayyun, and M. al-Mukhtar; software, N. Muhaisen; validation, N. Muhaisen, T. Khayyun, and M. al-Mukhtar.; formal analysis, N. Muhaisen, T. Khayyun, and M. al-Mukhtar; investigation, N. Muhaisen, T Khayyun, and M. al-Mukhtar; resources, N. Muhaisen.; data curation, N. Muhaisen.; writing—original draft preparation, N. Muhaisen.; writing—review and editing, N. Muhaisen, T. Khayyun, and M. al-Mukhtar.; visualization, N. Muhaisen; supervision, T. Khayyun, and M. al-Mukhtar; project administration, N. Muhaisen. All authors have read and agreed to the published version of the manuscript.

Funding

This research received no specific grant from any funding agency in the public, commercial, or not-for-profit sectors.

Data availability statement

Not applicable

Conflicts of interest

All authors contributed equally to this work.

References

[1] N. Abbas, S.A. Wasimia, N. Al-Ansari, Assessment of Climate Change Impacts on Water Resources of Al-Adhaim, Iraq Using SWAT Model, Engineering, 8 (2016) 716-732. http://dx.doi.org/10.4236/eng.2016.810065

[2] M. Al-Mukhtar, V. Dunger, B. Merkel, Evaluation of the climate generator model CLIGEN for rainfall data simulation in Bautzen catchment area, Germany. Hydrol. Res., 45 (2014) 615–630. https://doi.org/10.2166/nh.2013.073

[3] X. Wang, T. Yang, B. Yong, V. Krysanova, P. Shi., Environmental effects of climate change in the source regions of the Yellow River, J. Glaciol. Geocryol., 15 (2014) 1183–1192. https://doi.org/10.3390/w15112104

[4] J. Si, J. Li, Y. Yang, X. Qi, J. Li, Z. Liu, M. Li, S. Lu, Y. Qi, C. Jin, L. Qi, B. Yi, Y. Wang, Evaluation and prediction of groundwater quality in the source region of the Yellow River, Water, 14 (2022) 3946. https://doi.org/10.3390/w14233946

[5] S. Hagemann, C. Chen, J. Haerter, J. Heinke, D. Gerten, & C. Piani, Impact of a statistical bias correction on the projected hydrological changes obtained from three gcms and two hydrology models, J. Hydrometeorol., 12 (2011) 556–578. https://doi.org/10.1175/2011JHM1336.1

[6] S. Dehghan, N. Salehnia, N. Sayari, & B. Bakhtiari, Prediction of meteorological drought in arid and semi-arid regions using PDSI and SDSM: A case study in Fars Province, Iran. J. Arid. Land, 12 (2020) 318–330. https://doi:10.1007/s40333-020-0095-5

[7] H. Birara, R. Pandey, & S. Mishra, Projections of future rainfall and temperature using statistical downscaling techniques in Tana Basin, Ethiopia. Sustainable Water Resour, Manage., 6 (2020). https://doi.org/10.1007/s40899-020-00436-1

[8] Z. Mohammed, & W. H. Hassan, Climate change and the projection of future temperature and precipitation in southern Iraq using a Lars-WG model, Model. Earth Syst. Environ., 8 (2022) 4205–4218. https://doi:10.1007/s40808-022-01358-x

[9] Y. Osman, N. Al-Ansari, M. Abdellatif, S. B. Aljawad, & S. Knutsson, Expected future precipitation in central Iraq using Lars-WG Stochastic Weather Generator, Engineering, 6 (2014) 948–959. https://doi:10.4236/eng.2014.613086

[10] D. Phuong, T. Duong, N. Liem, V. Tram, D. Cuong & N. Loi, Projections of future climate change in the vu Gia Thu Bon River Basin, Vietnam by using statistical downscaling model (SDSM), Water, 12 (2020) 755. https://doi:10.3390/w12030755

[11] S. Kavwenje, L. Zhao, L. Chen, & E. Chaima, Projected temperature and precipitation changes using the statistical downscaling model in the Shire River Basin, Malawi. Int. J. Climatol., 42 (2021) 400–415. https://doi:10.1002/joc.7250

[12] S. Munawar, M. Tahir, & M. Baig, Twenty-first century hydrologic and climatic changes over the scarcely gauged Jhelum River basin of Himalayan region using SDSM and RCPS, Environ. Sci. Pollut. Res., 29 (2021) 11196–11208. https://doi:10.1007/s11356-021-16437-2

[13] W. Chen, K.Chau, Intelligent manipulation and calibration of parameters for hydrological models, Int. J. Environ. Pollut., 28 (2006) 432. https://doi:10.1504/ijep.2006.011221

[14] J. Martinec, A. Rango, R. Roberts, Snowmelt Runoff Model (SRM) User's Manual; Agricultural Experiment Station Special Report 100; College of Agriculture and Home Economics: Las Cruces, NM, USA, 2008.

[15] M. Jajarmizadeh, S. Harun, & M. Salarpour, An assessment on base and peak flows using a physically-based model, Res. J. Environ Earth Sci., 5.(2013) 49–57.

[16] J. G. Arnold, D. N. Moriasi, P. W. Gassman, K. C. Abbaspour, M. J. White, R. Srinivasan, C. Santhi, R. D. Harmel, A. van Griensven, M. W. Van Liew, N. Kannan, M. K. Jha, SWAT: Model Use, Calibration, and Validation, American J Agric Biol Sci, 55 (2012) 1491-1508. https://doi:0.13031/2013.42256

[17] P. W. Gassman, M. R. Reyes, C. H. Green, J. G. Arnold, The Soil and Water Assessment Tool: Historical Development, Applications, and Future Research Direction, Trans. ASABE, 50 (2007) 1211–1250. https://doi.org/10.13031%2F2013.23637

[18] M.S. Al- Khafaji, M. Al-Mukhtar, & A. S. Mohena, Performance of SWAT Model for Long-Term Runoff Simulation within Al- Adhaim Watershed, Iraq. Int. J. Sci. Eng. Res., 8 (2017) 1510 – 1517.

[19] T. S. Khayyun, I. A. Alwan, A. M. Hayder, Hydrological model for Hemren dam reservoir catchment area at the middle River Diyala reach in Iraq using ArcSWAT model, Appl. Water Sci., 9 (2019) 1-15. https://doi.org/10.1007/s13201-019-1010-0

[20] E. Koltsida, N. Mamassis, K. Andreas, Hydrological modeling using the SWAT Model in urban and peri-urban environments: The case of Kifissos experimental sub-basin (Athens, Greece), J. Hydrol. Earth Syst. Sci., (2021) 1-24. http://doi.org/10.5194/hess-2021-482

[21] S. Marahatta, L. P. Devekota, D. Aryal, Application of SWAT in Hydrological Simulation of Complex Mountainous River Basin (Part I: Model Development), Water, 13 (2021) 1-15. https://doi.org/10.3390/w13111546

[22] O. Al-Kakey, M. Al-Mukhtar, S. Berhanu, & V. Dunger, Assessing CFSR climate data for rainfall-runoff modeling over an ungauged basin between Iraq and Iran, Kuwait J. Sci., 50 (2023) 405-414, https://doi.org/10.1016/j.kjs.2022.12.004

[23] N. Abbasa, S. A. Wasimia, N. Al-Ansari, & S. Baby, Recent Trends and Long-Range Forecasts of Water Resources of Northeast Iraq and Climate Change Adaptation Measures, J. Water, 10 (2018) 1562. https://doi.org/10.3390/w10111562

[24] A. Al- Hilo, F. Saeed, & N. Al-Ansari, Impact of Climate Change on Water Resources of Dokan Dam Watershed, J. Eng., 11 (2019) 464-474. https://doi.org/10.4236/eng.2019.118033

[25] P. Gassman, A. Sadeghi, & R. Srinivasan, Applications of the SWAT model special section: Overview and insights, J. Environ. Qual., 43 (2014) 1–8. https://doi.org/10.2134/jeq2013.11.0466

[26] V. Shinde, N. Kamlesh, B. Sachin, & S. Manjushree, Water Quality Assessment and Application of SWAT Model for Hydrologic Simulations in a Mined Watershed, Clim. Chang. Environ. Sustain., 2 (2017)111-121. http://dx.doi.org/10.5958/2320-642X.2017.00012.6

[27] Chaoyue Li, Haiyan Fang, Assessment of climate change impacts on the streamflow for the Mun River in the Mekong Basin, Southeast Asia: Using SWAT model, CATENA, 201 (2021) 105199. https://doi.org/10.1016/j.catena.2021.105199

[28] T. Hemrassi, M. Khadhroui, H. Habaieb, Hydrological modelling of stream flows in the Rmel watershed using SWAT model, J. new sci., Agriculture and Biotechnology, 12 (2017) 2684-2692.

[29] S. Samuel, A. Shaibu, & A. Raymond, Application of SWAT hydrological model for assessing water availability at the Sherigu catchment of Ghana and Southern Burkina Faso, HydroResearch 3 (2020) 124-133. https://doi.org/10.1016/j.hydres.2020.10.002

[30] B. Vilaysanea, K. Takaraa, L. Pingping, A. Inthavy, D. Weili, Hydrological stream flow modelling for calibration and uncertainty analysis using SWAT model in the Xedone river basin, Lao PDR, Procedia Environ. Sci., 28 (2015) 380 – 390. https://doi.org/10.1016/j.proenv.2015.07.047

[31] M. Al- Hadithi, A. Elaiwi, & K. Hassan, Management of natural Iraqi water resources, Aims and Challenges, 3rd international conference on sustainable engineering techniques, 881, 2020 ,012181. https://doi.org/10.1088/1757-899X/881/1/012181

[32] A. Al-Madhhachi, A. Khayyun, & K. Wafa, Hydrological Impact of Ilisu Dam on Mosul Dam; the River Tigris, J. Geosci., 10 (2020) 1-14. https://doi.org/10.3390/geosciences10040120

[33] Z. Zakaria, N. Al-Ansari, S. Knutsson, Historical and future climatic change scenarios for temperature and rainfall for Iraq, J. Civ. Eng. Archit., 7 (2013) 1574-1594. http://dx.doi.org/10.17265/1934-7359/2013.12.012

[34] S. Al-Khafaji, F. Saeed, Effect of DEM and land cover resolutions on simulated runoff of adhaim watershed by SWAT model, Eng. Technol. J., 36 (2018) 439–448. https://doi.org/10.30684/etj.36.4a.11

[35] Al- Dabbagh, Z. Optimum hydroelectric energy generated from Mosul dam reservoir based on inflow ranges. Thesis submitted to the University of Mosul in a Partial Fulfullment of the Requirements for the Degree of of Master in Water Resources Engineering Sciences/ Iraq, 2022.

[36] N. Saddique, M. Usman, C. Bernhofer, Simulating the impact of climate change on the hydrological regimes of a sparsely gauged mountainous basin, Northern Pakistan, Water, 11 (2019) 2141. https://doi.org/10.3390/w11102141

[37] G. Chakilu, S. Sándor, T. Zoltán, Change in stream flow of Gumara watershed, Upper Blue Nile Basin, Ethiopia under representative concentration pathway climate change scenarios, Water, 12 (2020) 3046. https://doi.org/10.3390/w12113046

[38] S. Jianhua, L. Jianming, L. Sujin, Q. Xuejiao,. Effects of climate change on surface runoff and soil moisture in the source region of the Yellow River, Water, 15 (2023) 2014. https://doi.org/10.3390/w15112104

[39] S. Mehan, T. Guo, M. Gitau, & D. Flanagan, Comparative study of different stochastic weather generators for long-term climate data simulation, Climate, 5 (2017) 26. https://doi.org/10.3390/cli5020026

[40] M. Gitau, S. Mehan, & T. Guo, Weather Generator effectiveness in capturing climate extremes, Environmental Processes, 5 (2018) 153–165. https://doi.org/10.1007/s40710-018-0291-x

[41] J.G. Arnold, D.N. Moriasi, P.W. Gassman, K.C. Abbaspour, M.J. White, R. Srinivasan, C. Santhi, SWAT: Model Use Calibration and Validation, Am. Soc. Agric. Biol. Eng., 55 (2012) 1491-1508.

[42] P. Gassman, R. Reyes, C. Green, J. Arnold , The Soil and Water Assessment Tool: Historical Development, Applications, and Future Research Directions. Trans, ASABE, 50 (2007) 1211–1250. https://doi.org/10.13031/2013.23637

[43] J. Williams, Flood routing with variable travel time or variable storage coefficients, Trans. Asabe, 12 (1969) 0100–0103. https://doi.org/10.13031/2013.38772

[44] Yang, J., Reichert, P., Abbaspour, K. C., Xia, J., & Yang, H. Comparing uncertainty analysis techniques for a SWAT application to the Chaohe Basin in China. J. Hydrol., 358 (2008) 1–23. https://doi.org/10.1016/j.jhydrol.2008.05.012

[45] Saeed, F.H. Climate Change Adaptation Multi-criteria Decision-Making Model for Conflict Resolution of Water Resources Allocation in Iraq. Thesis, University of Technology, 2022.

[46] L. Haitham, M. Al-Mukhtar, Assessment of future climate change impacts on water resources of Khabour River catchment, north of Iraq, Eng. Technol. J., 40 (2022) 695–709. https://doi.org/10.30684/etj.v40i5.1925

[47] Y. Wu, J. Chen, Analyzing the water budget and hydrological characteristics and responses to land use in a monsoonal Climate River basin in South China, Environ. Manage., 51 (2013) 1174–1186. https://doi.org/10.1007/s00267-013-0045-5

[48] R.S. Ahl, S.W. Woods, H.R. Zuuring, Hydrologic calibration and validation of Swat in a snow-dominated Rocky Mountain Watershed, Montana, u.s.a.[1], J. Am. Water Resour. Assoc., 44 (2008) 1411–1430. https://doi.org/10.1111/j.1752-1688.2008.00233.x

[49] D.N. Moriasi, J.G. Arnold, M.W .Van Liew, R.L. Bingner, R.D Harmel, T.L. Veith, Model evaluation guidelines for systematic quantification of accuracy in watershed simulations, Am. Soc. Agric. Biol. Eng., 50 (2007) 885–900. https://doi.org/10.13031/2013.23153